



Soot combustion improvement in diesel particulate filters catalyzed with ceria nanofibers

P.A. Kumar, M.D. Tanwar, S. Bensaid*, N. Russo, D. Fino

Department of Applied Science and Technology, Politecnico di Torino, Corso Duca degli Abruzzi 24, 10129 Torino, Italy

H I G H L I G H T S

- ▶ Ceria nanofibers were prepared and deposited on DPFs to promote soot combustion.
- ▶ The nanofiber arrangement enhances the number of soot-fiber contact points.
- ▶ CO₂ concentration and the pressure drop were recorded during soot ignition.
- ▶ Nanofibers showed an oxidation temperature reduction vs nanopowders obtained with SCS.
- ▶ This behavior could greatly improve DPF passive regeneration.

A R T I C L E I N F O

Article history:
Available online 16 July 2012

Keywords:
Diesel particulate filter
Soot oxidation
Ceria
Nanofiber
Morphology

A B S T R A C T

Ceria nanofibers were prepared and deposited on SiC diesel particulate filters (DPFs), aiming at improving the soot-catalyst contact conditions and promote soot combustion at lower temperatures than in the noncatalytic case. In particular, the nanofibers have been found to be very active with respect to other ceria catalyst morphologies, due to their arrangement in a network which enhances the number of soot-fiber contact points.

This effect was initially elucidated in a series of tests of soot temperature programmed combustion, which were carried out on the catalysts powders mixed with soot in loose contact conditions: a specific sub-set of nanofibers exhibited a 112 °C anticipation of the onset oxidation temperature (10% of total soot combustion) with respect to the non-catalytic test, and 38 °C with respect to ceria nanopowders obtained with the so-called Solution Combustion Synthesis (SCS).

The nanofibers were then supported on Alumina washcoated DPFs, which were loaded with soot for 1 h, and subsequently subjected to a progressive temperature increase to induce soot ignition. Both CO₂ concentration in the outlet gas, and the pressure drop, were recorded during these tests. The main advantage given by the nanofiber catalyzed DPF, with respect to the other investigated morphologies, was not related to the maximum rate of soot oxidation, which was similar for all ceria catalysts, but again to the onset temperature. In fact, the pressure drop curve started to decrease more than 50 °C before the DPF catalyzed with ceria through *in situ* SCS.

This behavior could greatly improve the soot oxidation activity especially for DPF passive regeneration purposes.

© 2012 Elsevier B.V. All rights reserved.

1. Introduction

Diesel Particulate Matter (PM) is a very complex aerosol system [1,2], which has been the focus of a number of studies regarding its effects on human health [3]. PM is mainly constituted by carbonaceous particles (often called soot), originated from the incomplete in-cylinder combustion of the fuel, with diameters ranging from few nanometers (10–20 nm) to up to hundreds of nanometers

(the particles exceeding few μm are a negligible fraction), and the most common ones are around 100–200 nm [1]. However, the carbonaceous fraction is only a component of PM [1,2]: the nucleation and aggregation of soot particles is also accompanied by the adsorption of gases and the condensation of vapors (condensed volatile hydrocarbons). Moreover sulfur compounds and metallic ashes are also part of PM.

PM emission reduction is a challenging technological step for diesel engines, and is being tackled in the framework of a strict regulation worldwide. Diesel particulate filters (DPFs) are the most common devices for the collection of particulate matter for

* Corresponding author. Tel.: +39 011 0904662; fax: +39 011 0904699.
E-mail address: samir.bensaid@polito.it (S. Bensaid).

on-board diesel exhaust after-treatment. The capture of the solid fraction present in the diesel engine emissions, is carried out through a physical entrapment, thus preventing its release into the atmosphere. The filtration occurs in monolith shaped reactors having a wall-flow structure. The filter cannot accumulate particles indefinitely, and needs to be thermally regenerated, which involves the *in situ* combustion of the trapped PM. Particle removal can be continuous (passive regeneration), during the normal DPF filtration activity, or periodical (active regeneration), through a temperature increase inside the DPF. This temperature rise is induced by the post-injection of a specific amount of fuel, which burns in a catalytic converter upstream of the DPF itself and heats up the flue gases entering the filter, until the trapped soot starts to ignite and is converted to oxidized gaseous products. Active regeneration is mandatory if gas thermal levels are not sufficient to ensure a passive regeneration.

Most DPFs perform a catalytically assisted regeneration: the scope of the catalyst is to lower the active regeneration temperature, and to allow a certain degree of passive regeneration at suitable engine points characterized by high exhaust gas temperatures, thus delaying the regeneration phase. The drawback of the DPF catalytic coating is the increased pressure drop as compared to the bare filter, due to the additional resistance to the gas flow opposed by the washcoat layer.

The catalytic coating is located on the porous walls of the filter, and is normally constituted by a washcoat on the top of which noble metals are deposited. Alternative catalysts, such as mixed oxides of transition metals, have also been the object of several studies [4,5]: in fact, despite their lower activity compared to noble metals, they are characterized by a considerably lower cost.

Among these catalysts, CeO₂ has been widely investigated as a catalyst for soot combustion [6–12]: the Ce⁴⁺/Ce³⁺ redox cycle confers the ability to adsorb gaseous O₂, thus forming active oxygen at the catalyst surface (O_{ads}), which can be transferred to the soot-catalyst interface by superficial diffusion. This mechanism coexists with a temporary storage of the adsorbed oxygen as bulk lattice oxygen, which is then delivered as active O_{ads} at the catalyst surface. The latter phenomenon explains the CeO₂ catalyst activity even in the absence of O₂ in the gas phase, at least until the oxide integrity is preserved [12]. The bulk oxygen uptake/release cycle can be fostered by doping CeO₂ with rare earth, alkali or transition metal oxides, in order to promote bulk oxygen mobility, therefore speeding-up the soot oxidation rate, and to increase the oxide stability [7–9,11,12].

As a matter of fact, both the availability of active O_{ads} at the catalyst surface, and the number of soot-catalyst contact points, participate to the overall catalytic soot oxidation rate [9].

In fact, it is established that when soot is mixed with a catalysts in a ball mill (tight contact), the oxidation rate is much higher than when soot and the same catalyst are mixed by a spatula (loose contact). The increased number of contact points in tight conditions is responsible for this higher activity. In situ microscopy studies of catalytic soot oxidation, carried out under realistic conditions of temperature and oxygen partial pressure, confirmed the relationship between the oxidation rate and the nature of the soot-catalyst contact [13].

However, under practical conditions occurring in a catalytic DPF, loose contact rather than tight contact is encountered [4]. In fact, good contact conditions are very difficult to be reached due to the different orders of magnitude of the soot particle and the catalyst cluster sizes, which clearly hinders the overall activity of the catalyst.

In this work, in order to improve the soot-catalyst interaction, the morphology of the catalyst itself was designed in the attempt to maximize the number of contact points. CeO₂ catalysts in the form of nanofibers were synthesized to this end: instead of having

a foamy morphology, peculiar of the Solution Combustion Synthesis (SCS) technique [10], with inner porosities hardly accessible to soot particles [11], nanofibers are characterized by a high surface to volume ratio, typical of nearly mono-dimensional geometrical structures. Nanofibers are randomly arranged in a network which enhances the number of soot-fiber contact points, still having a high open porosity and thus a low associated pressured drop.

CeO₂ nanofibers were tested for soot oxidation in the form of powders, in order to discriminate the effect of the fibrous morphology with respect to the one obtained with SCS, in particular at low temperatures, which are relevant for passive regeneration purposes.

The same experiments were conducted on CeO₂ nanofibers coated on a lab-scale DPF, which was then loaded with soot under real conditions, in order to check the activity of the fiber catalyst when the real interaction between the coated catalyst and the deposited soot particle occurs.

2. Experimental procedure

2.1. Powder catalyst synthesis, characterization and testing

The CeO₂ nanofibers were synthesized by the coprecipitation/ripening method [14,15]. A 1 M solution of Cerium precursor was prepared by dissolving Ce(NO₃)₃·6H₂O (Aldrich, 99%) in distilled water. A second solution, with different mole ratios of NaOH/citric acid (0.3, 0.6, 0.8 and 1.0) (Aldrich), was prepared in another beaker. Both solutions were mixed together in a separate beaker and then kept at 90 °C for 24 h until the fibrous precipitates were obtained. The morphology of the precipitates was influenced by the NaOH/citric acid ratio: either bundle of sticks, or elongated individual fibers, or even flakes, were produced by controlling this parameter. After the precipitates were aged, the supernatant solution was analyzed by means of AAS (atomic absorption spectroscopy) to confirm the complete precipitation of Ce³⁺. The precipitates were finally filtered and washed with distilled water, followed by drying and calcination at different temperatures, between 300 and 600 °C, for 3 h in air. An aging test at 800 °C, in air for 12 h, was also performed to check the morphology stability.

The fibrous powder catalysts were then characterized: X-ray diffraction (PW1710 Philips diffractometer equipped with a monochromator, Cu K α radiation) was used to check the achievement of the cerium oxide structure. A field emission scanning electron microscope (FESEM, Leo 50/50 VP Gemini column) was employed to analyze the morphology of the CeO₂ nanofibers, and to correlate it to the activity towards soot oxidation. Finally, the specific surface areas of the prepared catalysts were evaluated through BET analysis, using a Micromeritics ASAP 2010 analyzer.

The activity of the oxidation catalysts towards soot combustion was analyzed by means of temperature programmed combustion (TPC), which was carried out in a fixed-bed micro-reactor (a quartz tube, i.d. 5 mm, placed in an electric oven), according to the standard operating procedure described in [16]: an N₂ flow containing 10% of O₂, was fed at a constant rate of 100 Nml min⁻¹, to the fixed bed which was constituted by 50 mg of a mixture of carbon (Printex U) and powdered catalyst (1:9 on a mass basis), diluted with \approx 150 mg of inert silica. The resulting amounts of each species were the following: 45 mg of catalyst, 5 mg of soot and 150 mg of silica. The *loose contact* catalyst-carbon mixture was prepared by gently shaking it in a polyethylene vessel for at least 15 min: in fact, as previously mentioned, loose contact is representative of the real contact conditions that occur in a catalytic trap for diesel particulate removal [4]. The reaction temperature was controlled through a PID-regulated oven and varied from 200 to 700 °C at a 5 °C/min rate. The CO/CO₂ concentration in the outlet gas was measured via NDIR analyzers (ABB). The peak temperature T_p of the TPC plot

of the outlet CO₂ concentration was taken as an index of the catalytic activity. The onset ($T_{10\%}$) combustion temperature, defined as the temperature at which 10% of the initial soot is converted, was also considered in order to better discriminate the intrinsic catalytic activity of the prepared catalysts. This is particularly important in order to rank the catalyst activity vs its morphology, at low temperatures which could be viable for passive regeneration. In fact, the onset combustion temperature only depends on the catalytic reaction, in a reaction rate limited regime; whereas, at higher conversion degrees, other phenomena (for instance, mass transfer limitations) could influence the real hierarchy of the catalysts. The inaccuracy of the thermocouple is below 1–2% of the absolute temperature value.

2.2. Supported catalyst preparation and testing

The CeO₂ nanofibers showing the best catalytic activity towards soot oxidation were supported on a lab-scale DPF. The SiC wall-flow filter, which was used for this purpose, had the following geometrical characteristics: 3 cm in length, 1.2 cm in side (square section), 180 cpsi, and average porosity of 42%. The deposition of CeO₂ nanofibers on the surface of the filter inner channels has been performed through the two following methods:

- Method 1: the CeO₂ nanofibers prepared by co-precipitation/ripening (NaOH/citric acid molar ratio equal to 0.8, calcination temperature of 300 °C for 2 h in air) were dispersed in a 5% HNO₃ solution, acting as a binder between CeO₂ and the SiC surface. This slurry solution was then ball-milled for 4 h. Grinding was used to obtain small enough particles to facilitate deposition on the monolith. The DPF was successively dipped into the resulting slurry, which adhered to the inner channel surface of the channels. The excess of slurry remaining in the channels was forced out by blowing a controlled air flux through the filter. A final calcination step was performed at 600 °C for 3 h in air. The load of deposited catalyst was assessed by gravimetric analysis. This procedure was repeated until the amount of deposited CeO₂ fibers catalyst was 14 wt.%, referred to the bare filter weight.
- Method 2: the prepared CeO₂ nanofibers were deposited on Alumina washcoated DPF. First, a thin layer of γ -Alumina (Al₂O₃) was deposited at 10% of the total weight of the monolith, in order to improve the subsequent adhesion of the catalytic powder to the monolith, and to increase the specific surface area on which the active CeO₂ fiber catalyst was deposited. Alumina powder was ground in a ball mill for 24 h at room temperature after adding 3.5 % of HNO₃ to obtain a slurry, in order to create an acidic environment and thus facilitate the dispersion of the particles. The monolith samples were immersed in the slurry, after which they were withdrawn slowly and then dried at 200 °C. On the top of this layer, the CeO₂ was deposited by dipping the washcoated filter into a water solution containing the uncalcined fibers. Finally, a calcination step at 600 °C for 3 h was performed in air. The amount of deposited CeO₂ fibers catalyst was also in this case equal to 14 wt.%.

CeO₂ nanofiber activity was compared to the one of conventional CeO₂ nanopowders, *in situ* synthesized in the DPF by means of the SCS [10]. The ceramic support was dipped in the aqueous solution of the precursors (Cerium nitrate and urea) and then placed into an oven at 600 °C. The aqueous phase was rapidly brought to boil, the nitrate precursors mixture ignited and the synthesis reaction took place *in situ*. The specific amount of deposited CeO₂ nanopowder was close to the ones reached in the other two cases, being around 15 wt.% of the bare filter weight. All these catalyst loadings correspond to ca. 1.37 g of CeO₂ in our system.

The as-prepared catalyzed monoliths were canistered with vermiculite in a stainless steel reactor, and then loaded with soot through a synthetic soot generator (Aerosol Generator GFG-1000-PALAS), at an Argon flow rate of 6 Nl/min. The soot mass flow rate was 5 mg/h and the loading time was fixed to 1 h for all investigated DPF samples. Therefore, an average soot loading of 1.15 g/l_{filter} was achieved, corresponding to 3.65 mg/g_{fibers}. Synthetic soot was employed in order to achieve reproducible data (no hydrocarbons were emitted by this carbon source), since real diesel soot features would be indeed too much dependent on the ever-changing engine conditions. As a matter of fact, the presence of adsorbed hydrocarbons in real soot particles introduces a difficult predictability of the aggregation phenomena due to an enhanced sticking factor, while in the regeneration phase (not treated in this work) it determines the actual reactivity of the deposited cake layer. During soot loading, the pressure drop was measured upstream and downstream of the DPF.

The procedure to investigate the deposited cake layer features, both in the absence and presence of a catalytic layer on the channel surface of the filter, was based on images from field emission scanning electron microscopy (FESEM-Leo 50/50 VP with Gemini column), as described in detail in [17]: at the end of the loading process, the filter was peripherally cut at half of its axial length, and then gently broken into two segments. The DPF sections were then observed to characterize the morphology of the coated catalyst and of the deposited soot cake.

The catalytic activity of the DPF catalyzed with the CeO₂ nanofibers was tested in a temperature programmed combustion (TPC) apparatus, hosting the canistered filter inside the reactor, after its loading with the soot produced by the aerosol generator. The reactor temperature was controlled through a PID regulated oven and it was increased during a TPC run from 200 to 700 °C at a 5 °C/min rate with a gas flow of 10% O₂ in N₂, at a total flow rate of 3 Nl/min. The analysis of the reactor outlet gas was performed by means of a CO/CO₂ NDIR analyzer (ABB). The temperature of the gases out-flowing from the DPF was measured by a thermocouple placed close to the filter outlet. The temperature corresponding to the CO₂ concentration peak (T_p) was taken as an index of the catalytic activity of each tested catalyst: the lower the T_p value, the higher the catalytic activity.

The pressure drop evolution was also recorded during the test, and its evolution was directly related to the progressive soot oxidation occurring inside the filter. Although the pressure drop decrease is not a direct measurement of soot consumption, which might not be complete even at the end of the test due to the possible presence of dead zones inside the filter, the simultaneous CO₂ concentration measurement was used to correlate soot oxidation to the pressure drop decrease.

A TPC run was also performed in the absence of the catalyst in order to set a reference for comparison purposes.

3. Results and discussion

3.1. Powder catalyst characterization

Several CeO₂ nanofibers were synthesized by varying the NaOH/citric acid molar ratio: in particular, ratios of 0.3, 0.6, 0.8 and 1 were used to select the most appropriate morphology to our purpose. As has been reported in [15], a NaOH/citric acid molar ratio below 0.6 lead to the formation of sticks, characterized by an elongated structure but collected in thick bundles which makes inaccessible most of the available surface. Conversely, a NaOH/citric acid molar ratio around one generates a morphology closer to a flake than a filament, still having elongated stick-wise sub-structures. In-between, i.e. for a ratio equal to 0.8, a clear fibrous

structure was obtained, as depicted in Fig. 1. If one focuses on this specific case, the length of the fibers ranges from some μm to tens of μm , while the fiber diameter goes from ≈ 100 nm to few hundreds of nm.

Fig. 1 shows the morphology of the CeO_2 nanofibers synthesized with a $\text{NaOH}/\text{citric acid}$ molar ratio equal to 0.8, hereafter denoted as CeO_2 (0.8), which seems not to be considerably affected by the calcination temperature: in particular, 3 h lasting calcinations in air at 300°C and 600°C were performed, the latter being more adequate to the temperatures normally encountered inside the DPF. It is therefore encouraging that the fibrous structure does not collapse after this thermal treatment.

The effect of the calcination temperature was investigated through XRD; also in this case, the analysis has been reported only for the most relevant sub-set of CeO_2 nanofibers, i.e. the CeO_2 (0.8), in Fig. 2. It can be seen that the XRD spectrum of the CeO_2 (0.8) treated at 300°C shows a rather amorphous structure as compared to the more crystalline one of the sample calcined at 600°C , as can be observed from the peak corresponding to the fluorite structure of CeO_2 (JCPDS card No. 34-0394).

This apparent stability of the fibrous morphology with respect of the calcination temperature, at which actually corresponds a certain modification in the crystalline structure of the sample, was accompanied by a drastic variation in terms of specific surface areas (SSA). Hence, the CeO_2 (0.3), (0.6), (0.8) and (1) nanofibers, calcined at 300°C , were all characterized by high SSA, ranging from

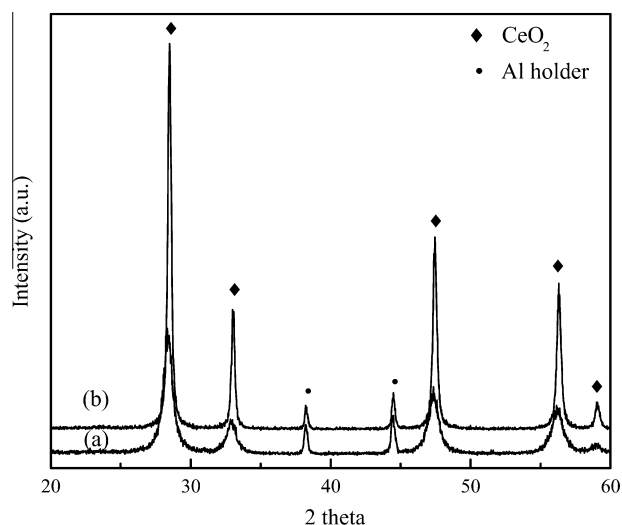


Fig. 2. XRD spectra of CeO_2 (0.8) fibers calcined at different temperatures: (a) 300°C and (b) 600°C .

107 to $120\text{ m}^2/\text{g}$. However, a higher calcination temperature lead to a strong SSA decrease in all tested samples. For instance, the CeO_2 (0.8) fibers calcined at 300°C had a SSA of $115\text{ m}^2/\text{g}$, which decreased to $21.5\text{ m}^2/\text{g}$ when the treatment was carried out at 600°C : the reason behind this strong decrease lies in the collapse of the smallest pores at the fiber surface, still preserving the main fibrous morphology of this prepared catalyst.

The catalytic activity tests which follow will enlighten the relationship between the morphological characteristics of the catalysts and their performances.

3.2. Powder catalyst activity

All prepared CeO_2 morphologies were tested towards the oxidation of soot in TPC runs, in order to select the structure which maximized the contact between soot and the catalyst itself.

Both tight contact and loose contact conditions were investigated. As previously mentioned in the introduction, tight contact forces the soot particle and the catalyst to be in intimate contact; generally, this analysis is used to discriminate the catalysts in terms of intrinsic activity, because soot oxidation is not rate-limited by a poor soot-catalyst contact. Loose contact conditions were also evaluated: in this case, the morphology of the catalyst plays a relevant role in determining the nature of the soot-catalyst contact.

Table 1 gathers the results of the performed TPC runs with CeO_2 catalysts calcined at 300°C : both the peak temperature (T_p) and the onset temperature ($T_{10\%}$) are here reported. All values refer to the conversion of soot to CO_2 , since the CO concentration was always almost negligible as compared to the one of CO_2 .

Starting from T_p , one can observe that all CeO_2 morphologies are considerably active in promoting soot combustion at temperatures well below the ones of non-catalytic combustion. In particular, for tight contact conditions, a very narrow interval of T_p was obtained for all catalyst, being around 400°C ; this means an anticipation of 200°C in the T_p of non-catalytic soot oxidation.

The same trend was noticed for the tests performed in loose contact conditions. Hence, although the T_p was 50°C higher on average with respect to the results obtained under tight contact, the reason of which has been attributed to the comparatively lower number of contact points, the morphology was not relevant in discriminating the various CeO_2 catalysts (all T_p were between 438°C and 447°C). In this regard, one can state that, when the soot oxidation rate is at its maximum value (corresponding to T_p in a CO_2 vs

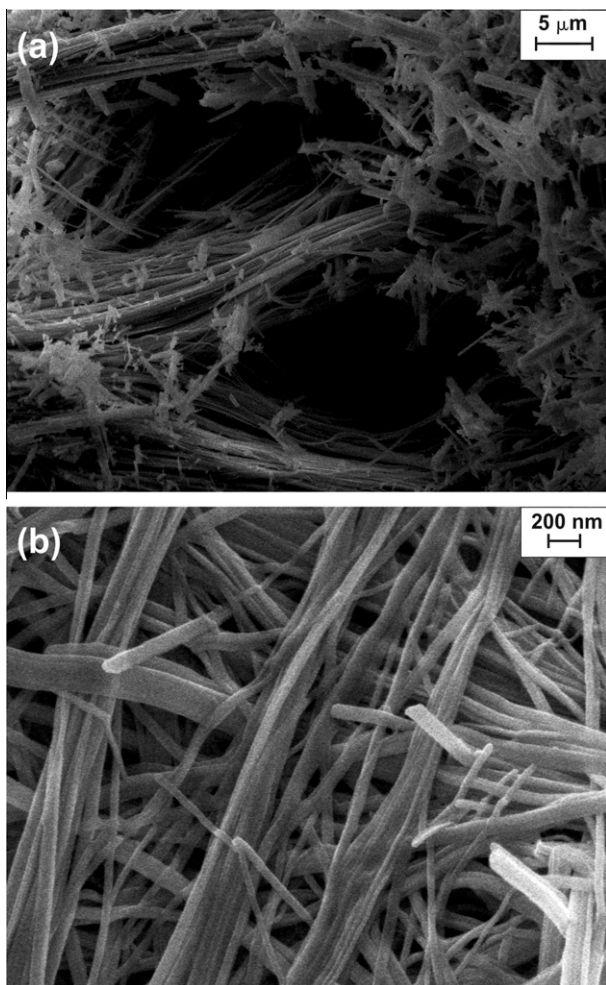


Fig. 1. FESEM images of CeO_2 (0.8) fibers calcined at different temperatures: (a) 300°C and (b) 600°C .

Table 1Soot combustion activity results, under loose and tight contact conditions, of CeO₂ nanofibers calcined at 300 °C and CeO₂ powders synthesized with SCS.

Catalyst	T_p tight contact (°C)	T_p loose contact (°C)	$T_{10\%}$ tight contact (°C)	$T_{10\%}$ loose contact (°C)
No-catalyst	600		470	
CeO ₂ nanofibers (0.3)	400	440	341	376
CeO ₂ nanofibers (0.6)	399	445	346	373
CeO ₂ nanofibers (0.8)	401	447	349	354
CeO ₂ nanofibers (1)	397	438	353	358
CeO ₂ with SCS	408	465	365	388

temperature plot), other factors than the number of contact points might be reaction rate-limiting for the soot oxidation, such as the oxygen availability at the soot-catalyst interface. The morphology is thus not decisive in these cases.

If one focuses on the onset temperatures, in our case fixed as 10% of the total soot conversion to CO₂, it is again clear that a remarkable advantage is obtained as compared to non-catalytic combustion. In case of tight contact conditions, a temperature decrease of around 120–130 °C was achieved, depending on the selected CeO₂ morphology. As for T_p , tight contact shades the effect of the morphology, due to the intimate soot-catalyst contact obtained by exerting an external mechanical force.

A totally different situation occurs for $T_{10\%}$ in loose contact conditions. In fact, CeO₂ (0.8) and (1) nanofibers are much more reactive than the other morphologies, as demonstrated by a ≈ 20 °C decrease in $T_{10\%}$ with respect to CeO₂ (0.3) and (0.6). This is probably due to the better accessibility of the catalyst surface to the soot particle; in other words, CeO₂ (0.8) reached an optimal match between the soot particle and catalyst fiber sizes, among the obtained morphologies.

This result is certainly not ascribed to the SSA, since all CeO₂ fibers were characterized by almost the same values.

The CeO₂ (0.8) nanofibers were also calcined at 600 °C: no considerable T_p increase was observed with respect to the results shown in Table 1, neither in tight (400 °C) nor in loose (445 °C) contact conditions [15]. This confirms that small scale porosities, which might collapse due to sintering and crystallite rearrangement at 600 °C treatments, are not so relevant in controlling the reaction rate of soot oxidation. Indeed, the fibrous network of the synthesized nanofibers seems to be at the grounds of the obtained soot oxidation activity (see Table 1).

A further aging of the CeO₂ (0.8) nanofibers at 800 °C in air, for 12 h, proved that the stability of the fibers was compatible with the temperatures occurring during soot oxidation: in fact, the T_p in tight and loose contact conditions were 409 °C and 457 °C, respectively [15], thus very close to the ones reported in Table 1.

All these results can be compared to the performance of powder CeO₂ obtained through SCS: in all cases, the CeO₂ nanofibers were slightly better towards soot oxidation; the only relevant improvement can be seen for $T_{10\%}$ in loose contact conditions (being of 34 °C between CeO₂ (0.8) nanofibers and SCS powders), where again the fibrous morphology seems to play a significant role in promoting a better soot-catalyst contact than does the foamy structure peculiar of SCS powders.

3.3. Supported catalyst characterization

FESEM direct observation of the deposited CeO₂ catalytic layer was performed. Figs. 3 and 4 depict the outcome of the two CeO₂ (0.8) fiber deposition methods, before any soot loading.

More specifically Fig. 3, refers to the catalytic coating obtained with the above-described Method 1. After several attempts, in which the grinding process and the calcination duration were optimized, it had been possible to bind the nanofibers to the bare SiC surface. However, two drawbacks characterized this deposition

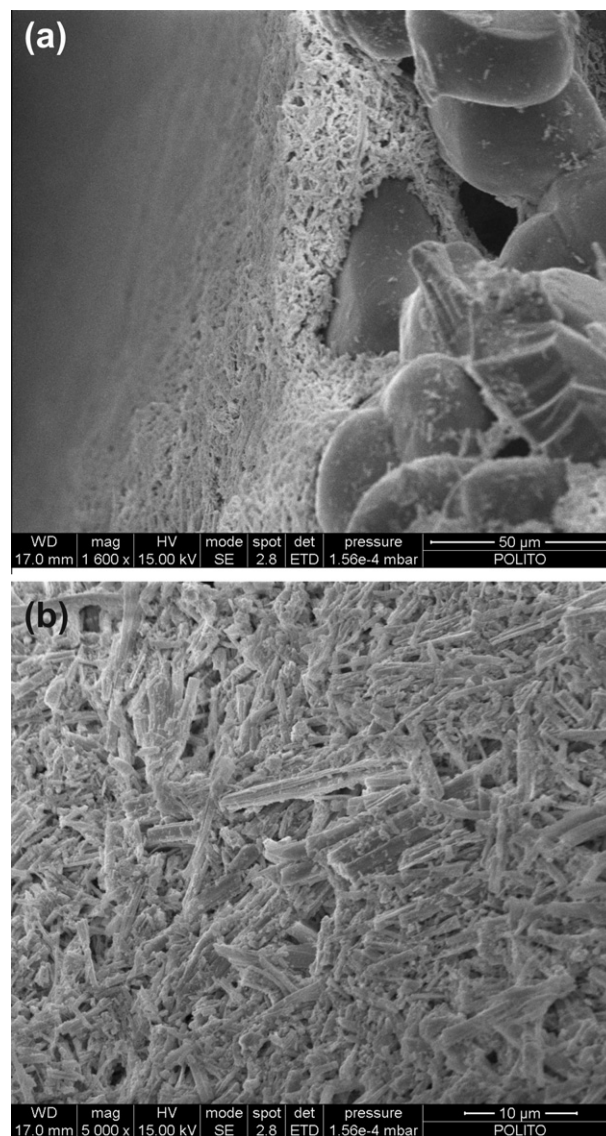


Fig. 3. FESEM images of CeO₂ (0.8) fibers synthesized, calcined and deposited on the DPF channel surface, according to Method 1.

method. The first one regards the fibers: in order to obtain a slurry that could easily flow and impregnate the whole axial length of the lab-scale DPF during dipping, an intense ball milling had to be operated, which however partially destroyed the original fibrous morphology. The second one is directly connected to the former: hence, the so-formed catalytic layer was very compact instead of being characterized by a high open porosity as initially expected. This generated a strong pressure drop across the filter, especially because a quite inhomogeneous catalyst loading occurred in the DPF channels, some of them being by far too much heavily loaded.

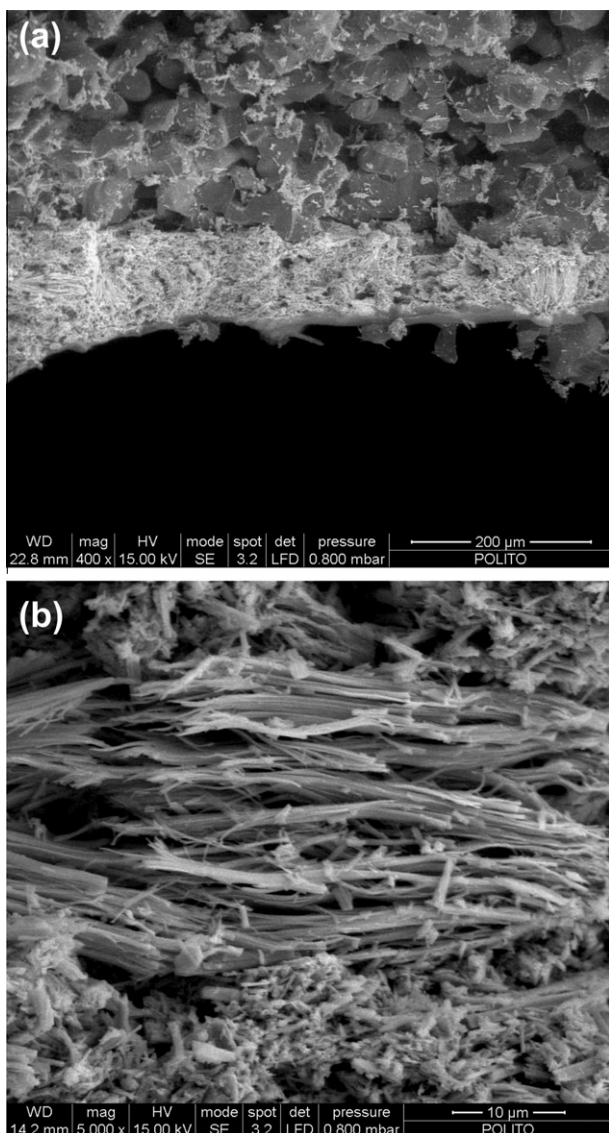


Fig. 4. FESEM images of CeO_2 (0.8) fibers synthesized, deposited on Alumina washcoat and *in situ* calcined on the DPF channel surface, according to Method 2.

On the other hand Fig. 4, reports the outcome of Method 2. In this case, the support for the fibers was given by the washcoat of Alumina, and no ball milling was required. The fibers were deposited by impregnating the washcoated DPF with the nanofiber solution, after which the calcination occurred *in situ*. In this way, the fibrous structure was totally preserved, and the arrangement of the catalytic layer was more suitable to the gas flow, as confirmed by the lower recorded pressure drop with respect to the former case. This was mainly due to a more even coating inside the DPF channels.

Fig. 5 depicts the structure of the cake layer in a cross section of the DPF, after the filter loading. In particular, the DPF was inspected at half of its axial length, where inlet or outlet perturbations are minimum. Both the bare filter and catalyzed one show the deposition of the soot cake on the top of the surface of the filter channels. From Fig. 5b it is difficult to assess the degree of penetration of soot into the fibrous structure: it is likely that part of the cake actually penetrates into the CeO_2 fibrous layer, but most of it appears to accumulate on the top of the catalytic surface. The contact points between soot and the layer of nanofibers can be clearly assimilated to a loose contact; therefore the maximization

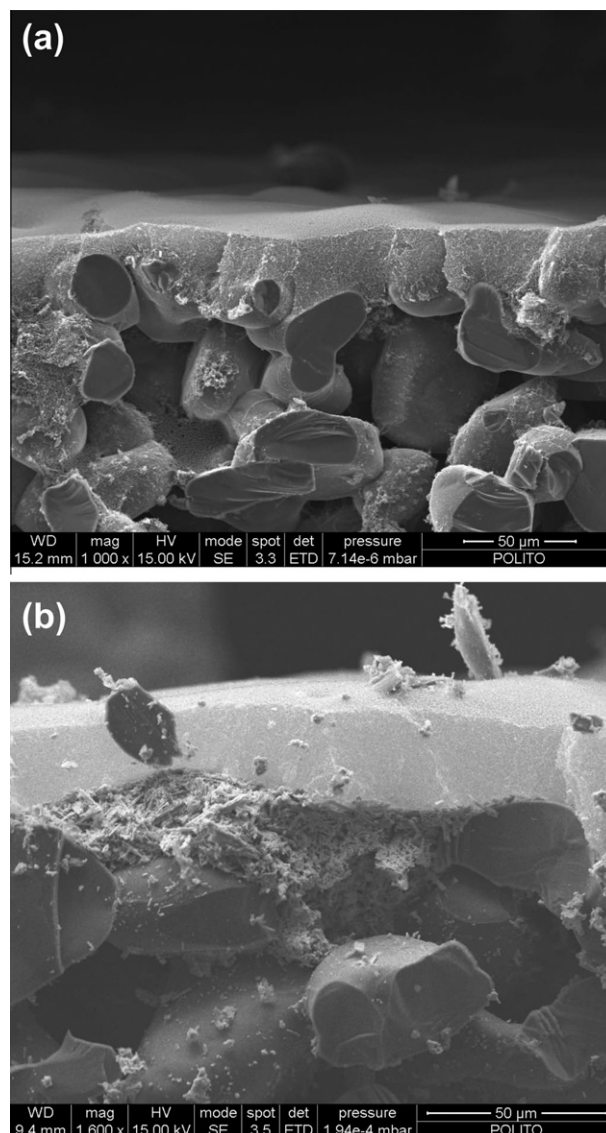


Fig. 5. FESEM images of the soot cake build-up on the top of (a) the bare DPF channel surface and (b) the CeO_2 (0.8) fiber layer, deposited according Method 2.

of the number of these contact points is extremely relevant, especially at low temperatures, in determining the soot oxidation rate.

3.4. Supported catalyst activity

Fig. 6 reports the pressure drop evolution during the soot loading test. The following samples were tested: a bare DPF; a catalyzed DPF with CeO_2 (0.8) nanofibers, deposited according to Method 1 (i.e. via monolith dipping into a slurry of calcined and ball milled nanofibers); a catalyzed DPF with CeO_2 (0.8) nanofibers, deposited according to Method 2 (i.e. via Alumina washcoated monolith dipping into an aqueous solution containing the dispersion of uncalcined nanofibers); a catalyzed DPF with a CeO_2 nanopowders deposited by *in situ* SCS.

It can be seen that the bare DPF is the one characterized by the slowest pressure drop increase; this is due to its poor filtration efficiency, which delays the formation of the soot cake. Hence, once the latter is built up, the slope of the curve is quite similar to one occurring in the other tests, since the soot layer, rather than the filter itself, becomes the real filtrating medium and reaches filtration efficiencies close to 1 [18].

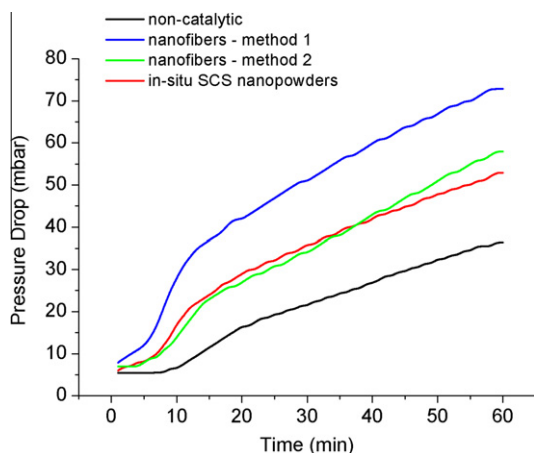


Fig. 6. Pressure drop evolution across the DPF during the soot loading phase, performed at ambient temperature, for a bare DPF (non-catalytic), a DPF with a catalytic layer of CeO_2 (0.8) nanofibers deposited according to Method 1 and Method 2, and a DPF coated with CeO_2 *in situ* synthesized with the SCS technique.

If one focuses on the curve referred to the CeO_2 (0.8) nanofibers deposited according to Method 1, one can see that the compactness of the catalytic layer, and its inhomogeneous distribution inside the filter channels along the axial coordinate (due to the viscosity of the slurry which did not adequately permeate the inner parts of the filter), conferred a very high filtration efficiency, as testified by the rapid pressure drop increase in the cake building phase. However, this is unsustainable if placed in the after-treatment line, because it would lead to an excessive resistance to the gas flow. Hence, all commercial monoliths and catalytic coatings have a porosity which is a compromise between filtration efficiency and gas flow resistance.

Finally, the CeO_2 (0.8) nanofibers deposited according to Method 2, and the CeO_2 nanopowders deposited by *in situ* SCS exhibited similar pressure drop evolutions. As previously mentioned, the steeper increase of the pressure drop is due to greater soot filtration capacity of these catalytic DPFs as compared to the bare one. Conversely, the initial pressure drop (i.e. of the clean filters) is more or less the same as the one of the bare DPF, which means that the coating is not detrimental to the initial resistance of the filter opposed to the gas flow. Although the soot generator provides a constant soot mass flow rate, a direct measurement of the deposited soot in the filter was not possible: in fact, a fraction of the soot particles in the flow sticks to the housing inner surfaces, or impacts and deposits at the front surface of the filter, instead of being trapped in the inner porosities of the DPF. This amount is not predictable, and cannot be directly assessed since the removal of the loaded filter from the housing, with the purpose of weighting it, would prevent the filter from being re-canistered. Hence, canistering occurs at temperatures above 600°C to enable vermiculite activation and expansion, which would also burn all the soot present in the filter.

The tubular reactor hosting the loaded filters was then directly transferred inside an oven, where the temperature was progressively increased to assess the catalyst activity towards soot oxidation. The loaded soot, exposed to a gas containing 10% of oxygen, as in common diesel exhaust flue gases, was progressively consumed: this behavior was followed by the evolving pressure drop across the filter, and by the CO_2 concentration at the DPF outlet. A thermocouple was positioned just downstream of the DPF, and it recorded the outlet gas temperature: it is worth mentioning that this is not the temperature occurring at the catalyst surface, which is much higher than the one recorded by the thermocouple. Therefore, the results of Fig. 7 should be considered only in comparative terms.

In Fig. 7, the normalized pressure drop was plotted against the temperature: in fact, as can be seen from Fig. 6, all loaded monoliths show a different pressure drop due to the different soot loadings and the presence/absence of the catalytic layer. In this way, the pressure evolution trends could be better compared. It can be seen that, at increasing temperature, all monolith samples exhibit the same pressure drop profile in the first part of the curve. The pressure drops were characterized by exactly the same slope for all samples, which is simply due to the viscosity increase of the gas, and its higher velocity inside the filter.

Then, the profiles start to differentiate, due to the individual features of soot combustion inside the DPFs. It can be seen that the uncatalyzed DPF shows a soot combustion interval, characterized by a relevant pressure drop decrease, between 330°C and 520°C . This temperature range is greatly modified by the presence of the CeO_2 catalytic coating.

In particular, the DPF catalyzed with CeO_2 (0.8) nanofibers deposited with Method 1 seems not to confer a substantial anticipation of soot oxidation: the pressure drop curve starts to decrease approximately at the same temperature of the uncatalyzed DPF, which means that the contribution of the catalyst at lower temperature is negligible. However, when the system slightly heats up, the effect of the CeO_2 catalytic coating is very active towards the oxidation reaction, as proven by the fact that soot is rapidly consumed until combustion completion (occurring at 460°C). One should bear in mind that a higher amount of soot was present in this DPF, catalyzed according to Method 1, than in any other tested DPF (see Fig. 6). This is probably the reason for the different slope of the pressure drop decrease during soot oxidation, with respect to the other catalyzed filters.

If one analyzes the behavior of the DPF catalyzed with *in situ* SCS synthesized CeO_2 , one notices that there is a slight anticipation (around 40°C) of the pressure drop decrease, ascribed to soot oxidation, with respect to the DPF catalyzed with CeO_2 (0.8) nanofibers deposited with the Method 1. This is certainly due to a good soot-catalyst contact, which has been previously discussed to be a relevant aspect in the oxidation of soot at low temperatures. After this “transitory”, the main chemical features of ceria, i.e. its ability to deliver active oxygen at the soot-catalyst surface, become dominant and, as for the T_p of the powder CeO_2 catalysts, no noticeable differences are detected between the various DPFs, regarding the temperature interval of the pressure drop decrease.

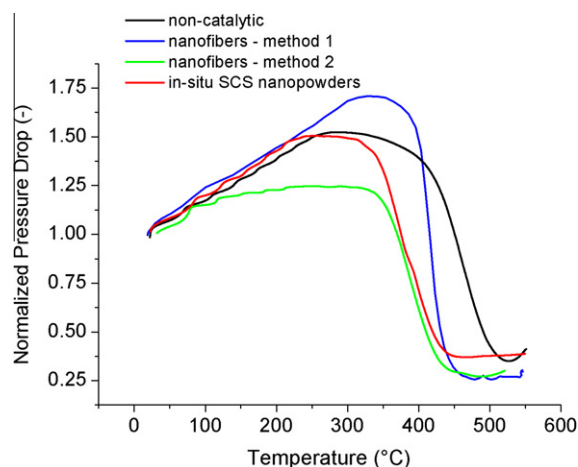


Fig. 7. Pressure drop evolution across the DPF during the soot oxidation phase, for a bare DPF (non-catalytic), a DPF with a catalytic layer of CeO_2 (0.8) nanofibers deposited according to Method 1 and Method 2, and a DPF coated with CeO_2 *in situ* synthesized with the SCS technique.

Finally, the analysis of the curve referred to the CeO₂ (0.8) nanofibers deposited with Method 2, suggests the occurrence of a substantially different phenomenon: the pressure drop curve bends well before all the other curves, and becomes almost flat for a quite large temperature interval (between 230 °C and 350 °C). This signifies that the soot oxidation rate generates a virtual pressure drop decrease, which is balanced by the increasing velocity of the flow, and thus its friction losses inside the filter. Although these temperatures are representative of the gas temperature, and not of the real temperature inside of the DPF, it is a remarkable result since this happens 150 °C before the uncatalyzed case, and more than 50 °C before the CeO₂ deposited by *in situ* SCS. This behavior is clearly attributed to the morphology of the catalyst, and to its capacity to entrap the soot particles in way that maximizes the number of contact points, at least in the proximity of the interface between the catalytic layer and the soot layer.

This is a very interesting finding since the morphology alone is responsible for this behavior, which confirms the results obtained in Table 1 with the nanofibers against the other morphologies. If we compare this result with the one of the DPF catalyzed according to Method 1, one can see that the latter is definitely not a suitable method to deposit the synthesized CeO₂ (0.8) nanofibers, because their highly porous and fibrous network was completely destroyed in the ball milling operation.

Finally, when CeO₂ entered in its suitable temperature range to show the highest activity, the morphology ceased to be the discriminating aspect, and the pressure drop decreased following the same trend observed for the other catalyzed DPFs.

A deeper insight in the real contribution of the catalyst to soot oxidation, in the unique soot-catalyst contact conditions occurring inside the DPF, can be derived from Fig. 8. In this figure, the CO₂ evolution during soot combustion was recorded, so that the temperature range of the pressure drop decrease could be associated to the soot-to-CO₂ oxidation. The experiments performed on the bare DPF and on the one catalyzed with CeO₂ (0.8) nanofibers according to Method 2, which proved to be the best way to preserve the fibrous structure even after calcination and deposition, are here reported.

The above-mentioned possible deviations in the amount of deposited soot inside the filter, from one loading test to the other one, which are also reflected by the slightly different integrals of the CO₂ curves, should not greatly affect the temperature at which soot oxidation occurs, due to the very low amount of oxidized soot as compared to the high thermal dilution effect given by gas flow rate.

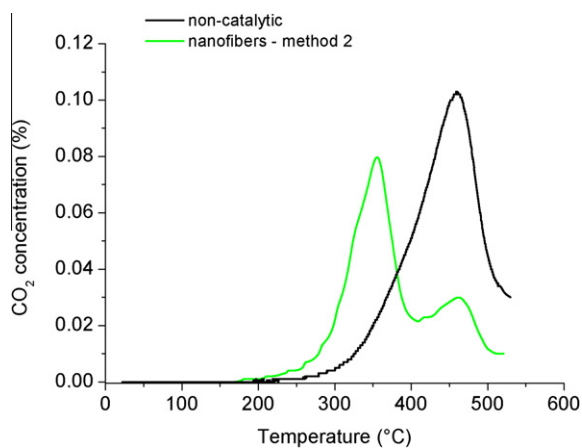


Fig. 8. CO₂ profiles during the soot oxidation phase for a bare DPF (non-catalytic) and a DPF with a catalytic layer of CeO₂ (0.8) nanofibers deposited according to Method 2.

It is worth noticing that the maximum slopes of the pressure drop decrease, observed in the two tests in Fig. 7, correspond to the CO₂ concentration main peaks depicted in Fig. 8. In reality, one can notice that the test with the CeO₂ (0.8) nanofibers deposited according to Method 2, show a double peak: the first and greater one in correspondence of the pressure drop decrease ascribed to the catalyst, while the second one is aligned to the one of non-catalytic combustion.

This CO₂ profile is peculiar of the soot combustion inside catalyzed DPFs, where part of the deposited soot is in contact with the catalytic layer, while part of it is inaccessible to the catalytic surface (as can be seen from Fig. 5b). Therefore, it happens that both catalyzed and uncatalyzed combustion occurs, and in this case the two phenomena can be clearly identified. This abstraction is known as two-layer model [19,20], and the deconvolution of the CO₂ concentration curve into the two contributions can be performed, in order to quantitatively assess the share of the catalytic oxidation with the respect to the overall amount of combusted soot. It has been estimated that 67% of soot was oxidized catalytically, while the remaining part occurred via the non-catalytic path.

The curve related to the CeO₂ (0.8) nanofibers, deposited according to Method 2, also shows that the slow and progressive pressure drop decrease occurring at low gas outlet temperatures (from 200 °C on, as visible in Fig. 7) was effectively due to soot combustion, which is demonstrated by the CO₂ presence, measured at the very same temperatures (Fig. 8).

It should be recalled that this behavior is particularly interesting in the sake of fostering the passive regeneration of the filter, thus delaying the active one and reducing the associated consumption of fuel.

4. Conclusions

Ceria-based catalysts for soot oxidation were investigated in this paper, with a specific focus on their morphology. In fact, soot combustion rate can be limited either by the oxygen availability at the soot-catalyst interface, which depends on the intrinsic activity of the catalyst in delivering active oxygen, or by the extension of the soot-catalyst interface itself. Since soot particles and the catalyst grain sizes often have different orders of magnitude, this leads to a poor accessibility of the soot particles to the catalyst inner porosities. This aspect could be rate-limiting especially at low temperatures.

For these reasons, CeO₂ nanofibers were obtained through the coprecipitation/ripening method, by controlling the pH using different NaOH/citric acid mole ratios, which lead to the formation of several kinds of structures, such as stick in bundle, fibers and flakes, as confirmed by FESEM images. The fibrous morphology (NaOH/citric acid = 0.8) was sought in the attempt to maximize the number of contact points between soot and the catalyst, by allowing a better penetration of soot in the network of nanofibers, which is characterized by a very high open porosity.

This concept was tested in soot oxidation tests. The most interesting finding was the following: while no major differences were noticed among all ceria catalysts in the tests performed in tight contact conditions, the catalyst morphology was quite relevant in loose contact ones. In particular, nanofibers promoted soot combustion at lower temperatures than the other kinds of structures, especially as far as the onset temperature ($T_{10\%}$) was concerned. CeO₂ nanofibers reduced by 112 °C the noncatalytic onset temperature, and by 38 °C the one of CeO₂ nanopowders obtained by Solution Combustion Synthesis (SCS). This proves that, when the ceria catalysts are intimately mixed to soot, they exhibit very close performances; whereas, if the soot-catalyst contact is limited, the morphology plays a relevant role, especially at low temperatures.

The CeO₂ nanofibers were then deposited on the channel surface of lab-scale DPFs, which were loaded with soot: in this way, the real contact conditions between the catalyst coating and the soot cake can be obtained, instead of resorting to the tight/loose concepts. The best deposition method involved a 10 wt.% Alumina washcoating, after which the DPF was impregnated by the uncalcined nanofiber suspension, and then a final thermal treatment in air at 600 °C for 2 h.

From soot combustion tests of the catalyzed monoliths, it has been found that no significant differences are noticed at the temperatures characterized by the highest oxidation activity, which occurred in correspondence of the steepest pressure drop decrease. However, the DPF coated with nanofibers anticipated by more than 50 °C the initial soot oxidation inside the filter with respect to the other morphologies (including the one obtained by *in situ* SCS), likely due to the better soot-catalyst contact conditions occurring inside the filter.

In order to fully understand this phenomenon, and to further improve the morphology of the catalytic layer, soot filtration and combustion should be investigated in different fluid-dynamic regimes and operating conditions.

References

- [1] M.M. Maricq, Chemical characterization of particle emissions from diesel engines: a review, *J. Aerosol Sci.* 38 (2007) 1079–1118.
- [2] I.M. Kennedy, Models of soot formation and oxidation, *Prog. Energy Combust. Sci.* 23 (1997) 95–132.
- [3] N. Englert, Fine particles and human health – a review of epidemiological studies, *Toxicol. Lett.* 149 (2004) 235–242.
- [4] J.P.A. Neef, M. Makkee, J.A. Moulijn, Catalysts for the oxidation of soot from diesel exhaust gases. I. An exploratory study, *Appl. Catal. B: Environ.* 8 (1996) 57–78.
- [5] G. Neff, L. Bonaccorsi, A. Donato, C. Milone, M.G. Musolino, A.M. Visco, Catalytic combustion of diesel soot over metal oxide catalysts, *Appl. Catal. B: Environ.* 11 (1997) 217–231.
- [6] A. Bueno-López, K. Krishna, M. Makkee, J.A. Moulijn, Active oxygen from CeO₂ and its role in catalysed soot oxidation, *Catal. Lett.* 99 (3–4) (2005) 203–205.
- [7] I. Atribak, A. Bueno-López, A. García-García, Thermally stable ceria-zirconia catalysts for soot oxidation by O₂, *Catal. Commun.* 9 (2008) 250–255.
- [8] I. Atribak, A. Bueno-López, A. García-García, Combined removal of diesel soot particulates and NO_x over CeO₂-ZrO₂ mixed oxides, *J. Catal.* 259 (2008) 123–132.
- [9] I. Atribak, F.E. López-Suárez, A. Bueno-López, A. García-García, New insights into the performance of ceria-zirconia mixed oxides as soot combustion catalysts. Identification of the role of “active oxygen” production, *Catal. Today* 176 (2011) 404–408.
- [10] P. Palmisano, N. Russo, D. Fino, C. Badini, High catalytic activity of SCS-synthesized ceria towards diesel soot combustion, *Appl. Catal. B: Environ.* 69 (1–2) (2006) 85–92.
- [11] E. Aneggi, C. de Leitenburg, G. Dolcetti, A. Trovarelli, Diesel soot combustion activity of ceria promoted with alkali metals, *Catal. Today* 136 (2008) 3–10.
- [12] E. Aneggi, C. de Leitenburg, A. Trovarelli, On the role of lattice/surface oxygen in ceria-zirconia catalysts for diesel soot combustion, *Catal. Today* 181 (2012) 108–115.
- [13] A. Setiabudi, N.K. Allaart, M. Makkee, J.A. Moulijn, In situ visible microscopic study of molten Cs₂SO₄-V₂O₅ – soot system: physical interaction, oxidation rate, and data evaluation, *Appl. Catal. B: Environ.* 60 (2005) 233–243.
- [14] J.Y. Yu, W.C.J. Wei, S.E. Lin, J.M. Sung, Synthesis and characterization of cerium dioxide fibers, *Mater. Chem. Phys.* 118 (2–3) (2009) 410–416.
- [15] P.A. Kumar, M.D. Tanwar, N. Russo, R. Pirone, D. Fino, Synthesis and catalytic properties of CeO₂ and Co/CeO₂ nanofibres for diesel soot combustion, *Catalysis Today* 184 (2012) 279–287.
- [16] D. Fino, N. Russo, G. Saracco, V. Specchia, The role of suprafacial oxygen in some perovskites for the catalytic combustion of soot, *J. Catal.* 217 (2003) 367–375.
- [17] S. Bensaid, D.L. Marchisio, N. Russo, D. Fino, Experimental investigation of soot deposition in diesel particulate filters, *Catal. Today* 147S (2009) S295–S300.
- [18] S. Bensaid, D.L. Marchisio, D. Fino, G. Saracco, V. Specchia, Modeling of diesel particulate filtration in wall-flow traps, *Chem. Eng. J.* 154 (1–3) (2009) 211–221.
- [19] M. Kostoglou, P. Housiada, A.G. Konstandopoulos, Multi-channel simulation of regeneration in honeycomb monolithic diesel particulate filters, *Chem. Eng. Sci.* 58 (2003) 3273–3283.
- [20] S. Lorentzou, C. Pagkoura, E. Papaioannou, M. Kostoglou, A.G. Konstandopoulos, K. Ohno, K. Ogyu, T. Oya, Catalyzed soot oxidation in diesel particulate filters: soot-catalyst interaction phenomena, in: *Third European Combustion Meeting, Chania-Crete (Greece)*, 11–13 April 2007.